Sound-field reproduction systems using fixed-directivity loudspeakers

M. Poletti
Industrial Research Ltd, P.O. Box 31-310, Lower Hutt 5040, New Zealand

F. M. Fazi and P. A. Nelson
Institute of Sound and Vibration Research, University of Southampton, Southampton SO17 1BJ, United Kingdom

(Received 30 November 2009; revised 30 March 2010; accepted 3 April 2010)

Sound reproduction systems using open arrays of loudspeakers in rooms suffer from degradations due to room reflections. These reflections can be reduced using pre-compensation of the loudspeaker signals, but this requires calibration of the array in the room, and is processor-intensive. This paper examines 3D sound reproduction systems using spherical arrays of fixed-directivity loudspeakers which reduce the sound field radiated outside the array. A generalized form of the simple source formulation and a mode-matching solution are derived for the required loudspeaker weights. The exterior field is derived and expressions for the exterior power and direct to reverberant ratio are derived. The theoretical results and simulations confirm that minimum interference occurs for loudspeakers which have hyper-cardioid polar responses.
 [DOI: 10.1121/1.3409486]

PACS number(s): 43.60.Tj, 43.55.Jz, 43.38.Md, 43.60.Sx [EJS] Pages: 3590–3601

I. INTRODUCTION

Sound reproduction systems attempt to produce sound arriving from arbitrary directions using arrays of loudspeakers. Many early systems used a small number of loudspeakers in a line in front of, or a circle around, the listener, and compensated for the limitation in the number of loudspeakers by including knowledge of psycho-acoustic effects.[1–4] With the use of larger numbers of loudspeakers, it became possible to reproduce sound pressure fields over a larger space using planar arrays[5–7] or 2D circular[8] or 3D spherical arrays.[9–18]

One of the limitations of implementing sound reproduction systems in rooms is that the room surfaces add unwanted early reflections and reverberation to the desired direct field produced by the loudspeakers.[19] These reflections may be reduced by acoustically treating the room. However, acoustic treatment may not be possible in many cases, and typically is difficult at low frequencies.

Active methods may be applied to reduce the influence of the room on the reproduced sound field.[12,19–26] Active compensation requires measurement of the loudspeaker responses at one or more receiving positions and the implementation of a digital compensator, which requires considerable processing. Furthermore, when the listener is present, the diffracted sound field from the listener will radiate out to the room surfaces and create secondary reverberation artifacts in the reproduction region. However, since these artifacts are typically of lower sound level than the reflections produced directly by the loudspeakers, compensation for first generation reflections can still produce a subjective improvement in sound quality.

There are two approaches which can offer reduced room influence without requiring active compensation and calibration. The simplest is to use loudspeakers with a fixed directivity which produces a reduced reverberant field. An array of directional loudspeakers will produce a direct sound which propagates through the listening region and reflects from wall surfaces on the far side of the array. The array will thus reduce early reflections from the nearest walls—which would produce tonal coloration—but the late echoes from far walls will still alter the spatial impression of the sound field.[27] A second approach is to use a loudspeaker array that creates a sound field within the array, but which prevents sound from radiating outward toward the room surfaces. This approach is described by the Kirchhoff-Helmholtz (K-H) integral formula, which shows that a sound field can be created within a region bounded by a surface S covered by an infinitely dense array of monopole and dipole sources normal to the surface S, and that the sound field outside the region is zero.[5–7,12–14,28–30] However, in practice a discrete array of loudspeakers must be used, and so the K-H solution can only be approximated at low frequencies.

A. Paper outline

This paper considers sound reproduction using fixed-directivity loudspeakers to reduce the influence of room acoustics. Each loudspeaker has a first-order response which is the weighted sum of a monopole and a radially-oriented dipole response, which allows the reverberant sound within the array to be reduced compared to the direct sound. The required loudspeaker weights are derived using a direct approach, and using a mode-matching approach which allows control of the reproduction error via regularization of a matrix inverse. The effect of reverberant sound level is quantified by calculating the direct to reverberant sound ratio produced by the loudspeaker array at the center of the reproduction region. This requires the derivation of the exterior power radiated from the array. It will be shown that at

 0001-4966/2010/127(6)/3590/12/$25.00

high frequencies the direct to reverberant ratio can be more simply written in terms of the directivity of the individual loudspeakers, and that the hyper-cardioid produces close to the maximum direct to reverberant ratio. The theory is evaluated using numerical simulations and the advantages and disadvantages of the two loudspeaker weight solutions are highlighted.

We commence with the spherical harmonic description of sound fields and monopole and dipole sources. Idealized forms of these sources will be used that represent the behavior of first-order loudspeakers with frequency-invariant polar responses.

II. SPHERICAL HARMONIC DESCRIPTION OF SOUND FIELDS

Let Ω_{r_L} be a sphere with radius r_L centered at the origin. A sound field is said to be an *interior* field if it satisfies the homogeneous wave equation in the interior of Ω_{r_L}, and it is conversely said to be an *exterior* field or a *radiating solution* if it satisfies the wave equation in the exterior of Ω_{r_L} and the Sommerfeld radiation condition.[28] This definition implies that all sources of sound and scattering objects are located in the interior of Ω_{r_L} for an exterior sound field, and outside the region for an interior field.

The solution to the wave equation can be expressed in spherical coordinates $\vec{r}=(r,\theta,\phi)$, where the arrow denotes a vector quantity, the vector norm $r=\|\vec{r}\|$ is the radial distance from the origin, θ is the elevation angle from the vertical z-axis and ϕ is the azimuthal angle from the x axis.[28] The general solutions for interior and exterior sound fields at negative frequency ω are[28]

$$p(r,\theta,\phi,k,t)=e^{-i\omega t}\sum_{n=0}^{\infty}\sum_{m=-n}^{n} j_n(kr)A_n^m(k)Y_n^m(\theta,\phi), \quad r<r_L \tag{1}$$

and

$$p(r,\theta,\phi,k,t)=e^{-i\omega t}\sum_{n=0}^{\infty}\sum_{m=-n}^{n} h_n(kr)C_n^m(k)Y_n^m(\theta,\phi), \quad r>r_L, \tag{2}$$

respectively, where $k=\omega/c$ rad/m is the wave number (the speed of sound c in m/s is assumed to be uniform in $\mathbb{R}^3$), $A_n^m(k)$ and $C_n^m(k)$ are the expansion coefficients, $j_n(x)$ is the nth order spherical Bessel function and $h_n(x)=h_n^{(1)}(x)$ is the nth order spherical Hankel function of the first kind. The spherical harmonic $Y_n^m(\theta,\phi)$ is defined as[30]

$$Y_n^m(\theta,\phi)=\sqrt{\frac{(2n+1)}{4\pi}\frac{(n-|m|)!}{(n+|m|)!}}P_n^{|m|}(\cos\theta)e^{im\phi}, \tag{3}$$

where $P_n^{|m|}(\cdot)$ is the associated Legendre function. The terms $j_n(kr)Y_n^m(\theta,\phi)$ and $h_n(kr)Y_n^m(\theta,\phi)$ are hereafter also referred as *modes* of the field.

Throughout this work, the assumption is made that the operating frequency ω and hence the wave number k are fixed.

A. Monopole and dipole sources

The acoustic pressure field generated by an ideal monopole source at $\vec{r}_s=(r_s,\theta_s,\phi_s)$ of unit amplitude in the free field (the free-space 3D Green function) is of the form[28]

$$p_m(\vec{r},\vec{r}_s,k)=G(\vec{r}|\vec{r}_s)=\frac{e^{ik\|\vec{r}-\vec{r}_s\|}}{4\pi\|\vec{r}-\vec{r}_s\|}. \tag{4}$$

The spherical harmonic expansion of the monopole field is given by[28]

$$p_m(\vec{r},\vec{r}_s,k)=\begin{cases} ik\sum_{n=0}^{\infty} j_n(kr)h_n(kr_s)\sum_{m=-n}^{n} Y_n^m(\theta,\phi)Y_n^m(\theta_s,\phi_s)^*, & r<r_s \\ ik\sum_{n=0}^{\infty} j_n(kr_s)h_n(kr)\sum_{m=-n}^{n} Y_n^m(\theta,\phi)Y_n^m(\theta_s,\phi_s)^*, & r>r_s. \end{cases} \tag{5}$$

The power of the monopole source of unitary amplitude is obtained by integrating the intensity over a sphere enclosing the source,[28] producing

$$W=\frac{1}{8\pi\rho c}, \tag{6}$$

where ρ is the density of air and ρc its characteristic impedance.

A dipole at position $\vec{r}_s$ and oriented in direction $\vec{v}$ has a field that takes the form[29]

$$p_d(\vec{r},\vec{r}_s,k)=\frac{\partial G(\vec{r}|\vec{r}_s)}{\partial\vec{v}}=-ik\frac{e^{ik\|\vec{r}-\vec{r}_s\|}}{4\pi\|\vec{r}-\vec{r}_s\|}\left[1+\frac{i}{k\|\vec{r}-\vec{r}_s\|}\right]\cos\gamma, \tag{7}$$

where γ is the angle between $\vec{v}$ and $\vec{r}-\vec{r}_s$. At large distances from $\vec{r}_s$, the dipole field tends to

$$p_d(\vec{r},\vec{r}_s,k)\to -ik\frac{e^{ik|\vec{r}-\vec{r}_s|}}{4\pi\|\vec{r}-\vec{r}_s\|}\cos\gamma, \quad \|\vec{r}-\vec{r}_s\|\gg\frac{1}{k}. \tag{8}$$

In order to produce a first-order directivity that is independent of frequency we equalize the dipole response by dividing by ik. The equalized dipole has the on-axis frequency response

$$|p_d(\vec{r},\vec{r}_s,k)|=\frac{1}{4\pi r}\sqrt{1+\frac{1}{(kr_d)^2}}, \tag{9}$$

where $r_d=\|\vec{r}-\vec{r}_s\|$. The near-field transition of the dipole occurs at $kr_d=1$, and the equalized response is flat for frequencies down to the transition frequency $f_d=c/(2\pi r_d)$, and rises at 6 dB/octave below that. Hence, to ensure flat responses down to a frequency f_L, we must maintain a distance from any equalized dipole greater than $r_d=c/(2\pi f_L)$.

The spherical harmonic expansion for a $1/(ik)$-equalized dipole oriented radially with respect to the origin is obtained from the derivative of Eq. (5) with respect to r_s as follows:

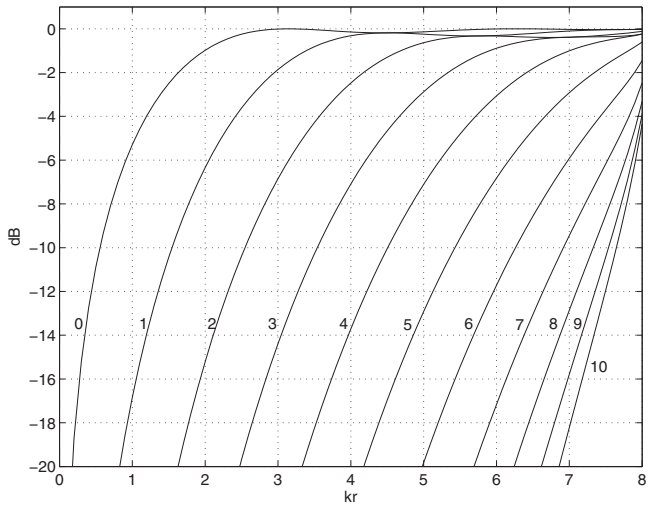

FIG. 1. Monopole truncation error for $kr_s=8$ and orders $N=0-10$.

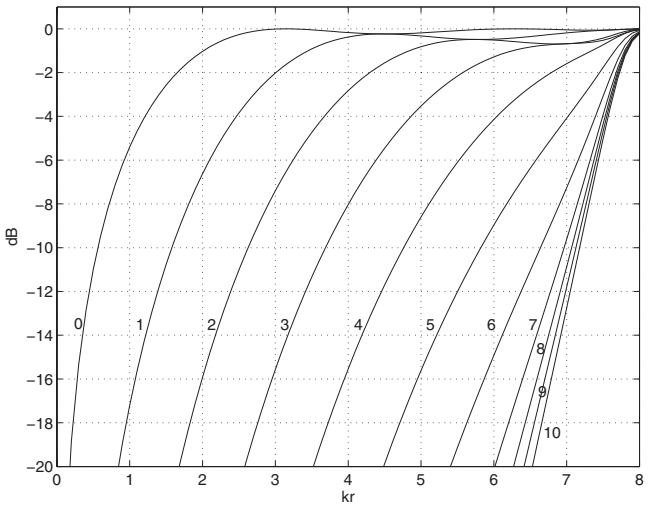

FIG. 2. Dipole truncation error for $kr_s=8$ and orders $N=0-10$.

$$p_d(r,\theta,\phi) = \begin{cases} k\sum_{n=0}^{\infty}\sum_{m=-n}^{n} j_n(kr)h_n'(kr_s)Y_n^m(\theta,\phi)Y_n^m(\theta_s,\phi_s)^*, & r<r_s \\ k\sum_{n=0}^{\infty}\sum_{m=-n}^{n} j_n'(kr_s)h_n(kr)Y_n^m(\theta,\phi)Y_n^m(\theta_s,\phi_s)^*, & r>r_s, \end{cases} \tag{10}$$

where $j_n'(\cdot)$ and $h_n'(\cdot)$ are the derivatives of the corresponding spherical Bessel and Hankel functions.

B. Truncation error of monopole and dipole field

In what follows we will be interested in the relative errors produced by the truncation of the monopole and dipole source expansions. The angle-averaged normalized truncation error for a monopole with order N expansion $p_T(r,\theta,\phi)$ is defined as[10,12]

$$\bar{\varepsilon}_{\mathrm{TM}}(N,kr) = \frac{\int_{\Omega_r} |p(r,\theta,\phi)-p_T(r,\theta,\phi)|^2 d\Omega_r}{\int_{\Omega_r} |p(r,\theta,\phi)|^2 d\Omega_r}, \tag{11}$$

where the overbar represent the average over all angles. Substituting the interior monopole expansions, Eq. (5) yields the interior monopole truncation error[12]

$$\bar{\varepsilon}_{\mathrm{TM}}(N,kr) = 1 - \frac{\sum_{n=0}^{N}(2n+1)j_n^{\,2}(kr)|h_n(kr_s)|^2}{\sum_{n=0}^{\infty}(2n+1)j_n^{\,2}(kr)|h_n(kr_s)|^2}, \quad kr<kr_s. \tag{12}$$

The truncation error is shown for $kr_s=8$ in Fig. 1. The error conforms approximately to the rule of thumb of -14 dB for $N=kr$ derived for plane waves in Ref. 4. However, for kr approaching kr_s higher order expansions are required to maintain accuracy. For example, a truncation error below -14 dB requires an order of $N=9$ at $kr=7$.

The interior truncation error for the dipole is found from Eq. (10) as follows:

$$\bar{\varepsilon}_{\mathrm{TD}}(N,kr) = 1 - \frac{\sum_{n=0}^{N}(2n+1)j_n^{\,2}(kr)|h_n'(kr_s)|^2}{\sum_{n=0}^{\infty}(2n+1)j_n^{\,2}(kr)|h_n'(kr_s)|^2}, \quad kr<kr_s. \tag{13}$$

This is shown in Fig. 2 for $kr_s=8$. For $kr \ll kr_s$ the error is around -16 dB for $N=kr$ but as kr approaches kr_s higher order expansions are again required. For example, $kr=7$ requires $N>10$ for -14 dB truncation error, a higher order than the monopole case.

C. Loudspeaker array geometry and Nyquist frequencies

We will assume a spherical array of loudspeakers, each of which can produce ideal monopole and dipole fields, at positions (r_L,θ_l,ϕ_l), $l\in[1,L]$ which approximate an equal sampling over the sphere, with numerical weighting coefficients β_l which allows accurate numerical integration (see for example Ref. 31).

A measure of the accuracy of the geometry is the cross correlation of the discretized spherical harmonics

$$\Gamma((n_1,m_1),(n_2,m_2)) = \sum_{l=1}^{L}\beta_l Y_{n_1}^{m_1}(\theta_l,\phi_l)Y_{n_2}^{m_2}(\theta_l,\phi_l)^*. \tag{14}$$

This is the discretized version of the orthogonality relation of the spherical harmonics.[28] For an ideal array $\Gamma((n_1,m_1),(n_2,m_2))=\delta_{n_1n_2}\delta_{m_1m_2}$ for all orders. However at high orders there will be insufficient samples to allow the orthogonality condition to be met. For example, Fig. 3 shows the cross correlation function for $L=144$ loudspeakers[31] and orders up to $N=11$. The error approaches 0 dB at large orders.

A second consequence of the discrete array is that it can only reproduce desired interior sound fields over a finite bandwidth. For the accurate representation of a monopole source field at radius r, Fig. 2 shows that the minimum order required is approximately $N=kr$. Since the exact control of $(N+1)^2$ modes requires at least as many loudspeakers, the

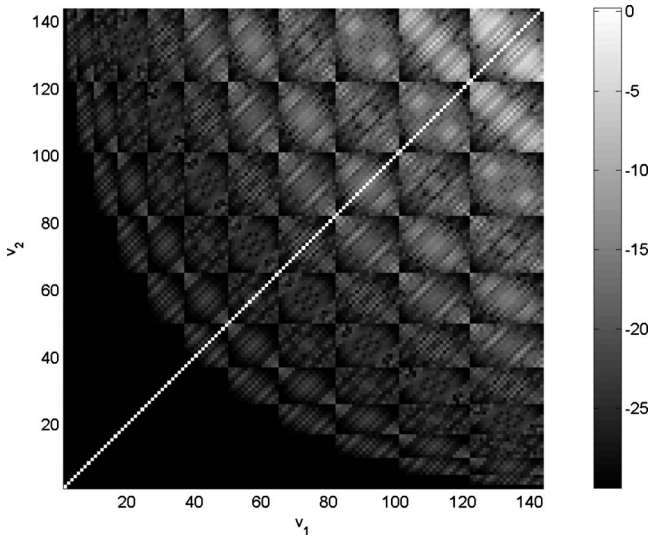

FIG. 3. Spherical harmonic cross correlation in dB, for $N=11$, $v_1=n_1^2+n_1+m_1+1$.

minimum number of loudspeakers required to represent the interior expansion of a first-order source of wave number k at radius r is approximately $L \geq (\lceil kr \rceil + 1)^2$ (see Ref. 10). If the loudspeakers are arranged uniformly or almost uniformly, it is reasonable to attempt the reproduction up to the frequency

$$f_{\mathrm{NI}}(r) = \frac{c(\sqrt{L}-1)}{2\pi r}. \tag{15}$$

This may be termed the interior Nyquist frequency, by the following simple argument: For a uniform spherical array of loudspeakers, the minimum angle between speakers is approximately $2\sqrt{\pi/L}$ rad. The sound rays from the loudspeakers to the origin at radius r are $2r\sqrt{\pi/L}$ apart. Setting this to a half wavelength yields approximately the same result as Eq. (15).

For $r=r_L$ the interior Nyquist frequency is such that the loudspeakers are half a wavelength apart and the interior Nyquist frequency is equal to the array's 'exterior' Nyquist frequency for generating an exterior field. This frequency will be important when calculating the reverberant field produced by the array (Sec. III E).

The interior and exterior Nyquist frequencies introduced here do not represent, as in the case of uniform sampling on an infinite line or on a circle, a precise boundary below which no artifacts due to spatial aliasing occur. Equation (15) is rather to be interpreted as an indicative upper frequency limit, below which the reproduction of the field can be expected to be accurate, under the ideal assumption of uniformly arranged speakers.[10]

III. SOUND REPRODUCTION SYSTEMS WITH FIXED-DIRECTIVITY LOUDSPEAKERS

An ideal first-order loudspeaker has a normalized, axially-symmetric polar response which is a weighted sum of monopole equation (4) and dipole equation (7) responses. The response using the equalized dipole may be written

$$p_a(\vec{r},\vec{r}_s,k) = \frac{e^{ik|\vec{r}-\vec{r}_s|}}{4\pi|\vec{r}-\vec{r}_s|}\left\{a-(1-a)\left[1+\frac{i}{k|\vec{r}-\vec{r}_s|}\right]\cos\gamma\right\}, \tag{16}$$

where $a \in [0,1]$ is the first-order weighting parameter and γ is the angle from the loudspeaker axis. The corresponding spherical harmonic expansion of the first order source is, from Eq. (5) and Eq. (10),

$$p_a(\vec{r},\vec{r}_s,k) = \begin{cases} k\sum_{n=0}^{\infty}\sum_{m=-n}^{n} j_n(kr)[iah_n(kr_s)+(1-a)h_n'(kr_s)]Y_n^m(\theta,\phi)Y_n^m(\theta_s,\phi_s)^*, & r<r_s \\ k\sum_{n=0}^{\infty}\sum_{m=-n}^{n} h_n(kr)[iaj_n(kr_s)+(1-a)j_n'(kr_s)]Y_n^m(\theta,\phi)Y_n^m(\theta_s,\phi_s)^*, & r>r_s. \end{cases} \tag{17}$$

The distance-scaled far-field response of the first order source is, from Eq. (16),

$$q(\gamma) = a-(1-a)\cos\gamma. \tag{18}$$

For $a=1$ the loudspeaker is omnidirectional and for $a=0$ it produces a dipole response. The directivity, $D(a)$, of the first-order loudspeaker[32,33] then follows the same analysis that has been applied to first-order microphones[34] and is given by

$$D(a) = \frac{4\pi}{2\pi\int_0^{\pi}|q(\gamma)|^2\sin\gamma d\gamma} = \frac{3}{3a^2+(1-a)^2}. \tag{19}$$

This has a value of 3 for $a=0.5$ (the cardioid response) and has a maximum value of $D(a)=4$ for $a=0.25$ (the hypercardioid response). Higher directivities can be obtained using second-order loudspeakers, or arrays of loudspeakers. Note that in the near-field, $k\|\vec{r}-\vec{r}_s\|<1$, the equalized dipole magnitude increases and the first-order response in Eq. (18) is no longer correct. The directivity D of a source implies that the sound at a distance r on-axis will be D times the average intensity the source produces at the same distance r. Equivalently, the average power radiated from the source is $1/D$ times the power radiated through a small area on-axis.

A. Direct solution for fixed-directivity loudspeaker weights

Consider a continuous distribution of monopole and

radially-oriented, equalized dipole speakers on the surface of a sphere Ω_{r_L} of radius r_L at positions $\vec{r}_v=(r_L,\theta_v,\phi_v)$, $\theta_v \in [0,\pi]$ and $\phi_v \in [0,2\pi]$. The interior sound field at position $\vec{r}$ can be written

$$p(\vec{r}) = \int_0^{\pi}\int_0^{2\pi}\left[aG(\vec{r}|\vec{r}_v) - \frac{(1-a)}{ik}\frac{\partial}{\partial\vec{n}(\vec{r}_v)}G(\vec{r}|\vec{r}_v)\right] \times w(\theta_v,\phi_v)\sin\,\theta_v d\theta_v d\phi_v, \quad r<r_L, \tag{20}$$

where $\vec{n}(\vec{r}_L)$ is the unitary vector normal to Ω_{r_L} at $\vec{r}_v$ and directed toward its exterior. Since the weights $w(\theta_v,\phi_v)$ are a function of (θ_v,ϕ_v) they have the general form[28]

$$w(\theta_v,\phi_v) = \sum_{n=0}^{\infty}\sum_{m=-n}^{n} Q_n^m Y_n^m(\theta_v,\phi_v), \tag{21}$$

where Q_n^m are the expansion coefficients. Substituting the interior form of the monopole and equalized dipole expansions, Eq. (5) and Eq. (10), and the assumed weight solution Eq. (21) into Eq. (20) and employing the orthogonality of the harmonics yields

$$p(\vec{r}) = k\sum_{n=0}^{\infty}\sum_{m=-n}^{n} j_n(kr)Q_n^m[aih_n(kr_L)+(1-a)h_n'(kr_L)] \times Y_n^m(\theta,\phi). \tag{22}$$

This must equal the interior expansion of the general sound field in Eq. (1). Hence

$$Q_n^m = \frac{A_n^m}{k[aih_n(kr_L)+(1-a)h_n'(kr_L)]} \tag{23}$$

and the continuous distribution of weights is

$$w(\theta_v,\phi_v) = \sum_{n=0}^{\infty}\sum_{m=-n}^{n}\frac{A_n^m Y_n^m(\theta_v,\phi_v)}{k[aih_n(kr_L)+(1-a)h_n'(kr_L)]}. \tag{24}$$

For $a=1$, this solution is the simple source solution for monopole reproduction.[12,18,28,35,36]

For a discrete array, with loudspeaker angles (θ_l,ϕ_l), $l \in [1,L]$, and weighting coefficients β_l, the discrete loudspeaker weights truncated to order N are

$$\hat{w}_l = \beta_l\sum_{n=0}^{N}\sum_{m=-n}^{n}\frac{A_n^m Y_n^m(\theta_l,\phi_l)}{k[aih_n(kr_L)+(1-a)h_n'(kr_L)]}, \quad l \in [1,L]. \tag{25}$$

The weights are required so that the reproduction using L loudspeakers implements the discrete approximation to Eq. (20). For a point source, Eq. (5), located in the exterior of Ω_{r_L}, the loudspeaker weights are obtained by substituting the interior expansion coefficients $A_n^m=ikh_n(kr_s)Y_n^m(\theta_s,\phi_s)^*$. Note that the solutions in Eq. (25) are in general a function of frequency, and therefore represent weighting filters, with associated impulse responses in the time domain. The solutions must be calculated at discrete frequencies spaced at $\Delta f=1/\tau$ to represent the corresponding loudspeaker impulse responses over their approximate time duration τ. The impulse response is then obtained via an inverse discrete Fourier transform. Sample rates less than Δf will lead to time-aliasing of the impulse response.[37]

For the continuous array, we can also calculate the exterior field using the exterior field forms of Eq. (5) and Eq. (10), with the weight function in Eq. (24) yielding[37]

$$p(\vec{r}) = \sum_{n=0}^{\infty}\sum_{m=-n}^{n} A_n^m(k)\left[\frac{aj_n(kr_L)+i(1-a)j_n'(kr_L)}{ah_n(kr_L)+i(1-a)h_n'(kr_L)}\right] \times h_n(kr)Y_n^m(\theta,\phi), \quad r>r_L. \tag{26}$$

This will be used to calculate the reverberant field produced by the array in Sec. III E., Note that the exterior forms in Eq. (5) and Eq. (10) mean that the above expression includes the sound that propagates across the interior of the array and out the other side.

B. Mode-matching solution

An alternative approach to the analytical solution above is obtained by requiring that the modal decomposition of the sound field produced by the loudspeakers match that of the desired sound field.[12] For an arbitrary field with coefficients A_n^m, using Eqs. (1), (5), and (10) and the orthonormality property of the spherical harmonics this produces, for each n and m, and with mode matching weights $\bar{w}_l$,

$$k\sum_{l=1}^{L}\bar{w}_l[iah_n(kr_L)+(1-a)h_n'(kr_L)]Y_n^m(\theta_l,\phi_l)^* = A_n^m. \tag{27}$$

This can be written in matrix form

$$\mathbf{\Psi}_F\mathbf{w} = \mathbf{H}_a\mathbf{Y}\mathbf{w} = \mathbf{d}, \tag{28}$$

where $\mathbf{\Psi}_F$ is a K by L matrix $(K=(N+1)^2)$, $\mathbf{w}$ is an L by 1 vector of loudspeaker weights $\bar{w}_l$, and $\mathbf{d}$ is a K by 1 vector of desired field coefficients $\mathbf{d}(b)=A_n^m$.

The matrix $\mathbf{\Psi}_F$ can be factored into the K by K diagonal matrix $\mathbf{H}_a$ with elements $H_a(b,b)=k[iah_n(kr_L)+(1-a)h_n'(kr_L)]$, where $b=n^2+n+m+1$, and a K by L matrix $\mathbf{Y}$ of spherical harmonic terms $Y(b,l)=Y_n^m(\theta_l,\phi_l)^*$. Note that $\mathbf{H}_a$ contains $2n+1$ repeated elements for each n.

For $K \geq L$ the vector of mode matching weights which produces the minimum squared error is[10,38]

$$\mathbf{w} = [\mathbf{\Psi}_F{}^H\mathbf{\Psi}_F + \lambda_F\mathbf{I}]^{-1}\mathbf{\Psi}_F{}^H\mathbf{d}, \tag{29}$$

where λ_F is an optional regularization parameter and superscript H denotes the conjugate transpose.

For $K<L$ the mode matching weights are found from the minimum energy solution[10,39]

$$\mathbf{w} = \mathbf{\Psi}_F{}^H[\mathbf{\Psi}_F\mathbf{\Psi}_F{}^H + \lambda_F\mathbf{I}]^{-1}\mathbf{d}, \tag{30}$$

where λ_F allows the energy to be reduced below the minimum energy solution, with a corresponding increase in error.

As for the solution in Eq. (25), the solutions in Eqs. (29) and (30) are in general frequency-dependent and must be calculated at a frequency spacing Δf which prevents temporal aliasing of the corresponding filter impulse responses.

C. Comparison of solutions

The similarities between the direct and mode matched solutions may be made clearer by writing Eq. (28) as $\mathbf{Yw}=\mathbf{H}_a^{-1}\mathbf{d}$ (since $\mathbf{H}_a$ is square). The mode matched solution can then be written

$$\mathbf{w}=\begin{cases}[\mathbf{Y}^H\mathbf{Y}+\lambda_F\mathbf{I}]^{-1}\mathbf{Y}^H\mathbf{H}_a^{-1}\mathbf{d}, & K\geq L\\ \mathbf{Y}^H[\mathbf{Y}\mathbf{Y}^H+\lambda_F\mathbf{I}]^{-1}\mathbf{H}_a^{-1}\mathbf{d}, & K<L,\end{cases} \tag{31}$$

and the direct solution in Eq. (25) may be written in a similar matrix form as

$$\hat{\mathbf{w}}=\mathbf{B}\mathbf{Y}^H\mathbf{H}_a^{-1}\mathbf{d}, \tag{32}$$

where $\mathbf{B}$ is an L by L diagonal matrix of weighting coefficients β_l. It is now apparent that the mode matching solution contains an additional inverse matrix which compensates for the non-orthogonality of the loudspeaker spherical harmonic matrix, whereas the direct solution uses a weighting vector proportional to the solid angle associated with each loudspeaker, but does not compensate for non-orthogonality.[12]

D. Robustness

The solutions derived above require that all loudspeakers have identical polar responses. Furthermore, the loudspeakers must be positioned exactly at (r_L,θ_l,ϕ_l) for the spherical harmonic matrix $\mathbf{Y}$ to be valid. In practice, neither of these conditions can be met precisely, and therefore, there will be an additional error in the reproduced field above the solution error $\|\mathbf{\Psi}_F\mathbf{w}-\mathbf{d}\|^2$, due to errors in $\mathbf{\Psi}_F$.[40] The sensitivity of the solution to these errors is governed approximately by the condition number of $\mathbf{\Psi}_F$.[41]

The approximate condition number of $\mathbf{\Psi}_F$ for $K<L$ may be derived as follows. For $K<L$ the matrix $\mathbf{\Psi}_F$ has a singular decomposition $\mathbf{\Psi}_F=\mathbf{U}\mathbf{S}_K\mathbf{V}^H$ where $\mathbf{U}$ is a K by K unitary matrix, $\mathbf{S}_K$ is a K by L matrix containing (at full rank) K singular values $[\sigma_1,\sigma_2,\ldots,\sigma_K]$, and $\mathbf{V}$ is an L by L unitary matrix.[38]

The squared singular values of $\mathbf{\Psi}_F$ are the eigenvalues of

$$\mathbf{\Psi}_F\mathbf{\Psi}_F{}^H=\mathbf{U}\mathbf{S}_k^2\mathbf{U}^H=\mathbf{H}_a\mathbf{Y}\mathbf{Y}^H\mathbf{H}_a{}^H\approx\mathbf{H}_a\mathbf{H}_a{}^H, \tag{33}$$

assuming that $\mathbf{Y}\mathbf{Y}^H\approx\mathbf{I}$. Hence the $2n+1$ repeated singular values are approximately

$$\sigma_n=|aih_n(kr_L)+(1-a)h_n'(kr_L)|, \tag{34}$$

and so the condition number is

$$\kappa_F=\frac{|aih_N(kr_L)+(1-a)h_n'(kr_L)|}{|aih_0(kr_L)+(1-a)h_0'(kr_L)|}=(kr_L)^2\frac{|aih_N(kr_L)+(1-a)h_n'(kr_L)|}{[(kr_L)^2+(1-a)^2]^{1/2}}. \tag{35}$$

The condition numbers are shown for an array of 144 loudspeakers at a radius 1.5 m at four frequencies from 100 to 600 Hz in Fig. 4. The match is good for $K<L$ $(N<11)$ as expected, but at 200 and 300 Hz the theoretical value is also approximately true for $K>L$. For $K=L$ there is an increase in condition number at all frequencies, which is most apparent above the exterior Nyquist frequency of the array (400 Hz). The condition number behavior above the Nyquist frequency is similar to that of the condition number of random normal matrices,[42] which has a peak when the matrix is square. The distributions of the real and imaginary parts of the entries in $\mathbf{\Psi}_F$ are not normal, and so the precise variation of the log of the condition number does not follow that in Ref. 42, but the peak value at $K=L$ is similar to the value $E\{\log(\kappa_F)\}=\log(L)+0.982$ (5.95 for $L=144$) derived in Ref. 42.

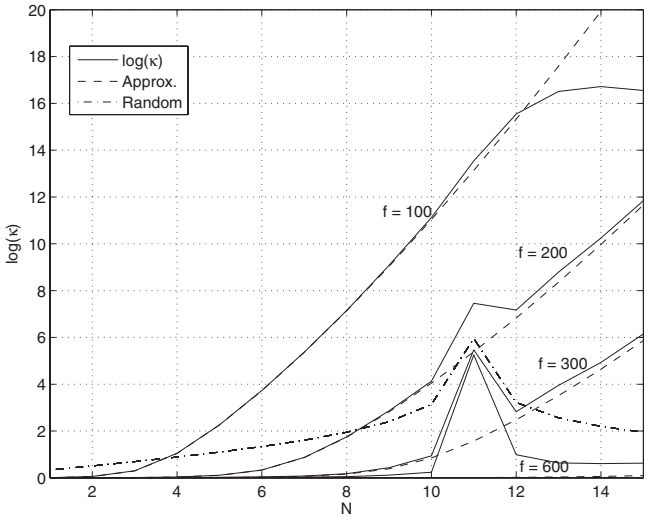

FIG. 4. $\log(\kappa)$ calculated at 4 frequencies, $K<L$ approximation from Eq. (35) and random normal matrix result, $L=144$, $r_L=1.5$ m.

E. Direct to reverberant ratio

The optimum directivity of the loudspeakers in a sound reproduction system depends on the acoustic parameter to be optimized. If the goal is to minimize the level of the reverberant sound at the center of the array, the optimum is obtained by maximizing the ratio of the direct sound to the reverberant sound at the center of the array. We briefly review the derivation of the direct to reverberant ratio (DRR) here.

1. DRR for a single loudspeaker

If a directional loudspeaker with directivity D, emitting acoustic power W_l is placed in a semi-reverberant room, then at a distance r_L, on-axis, the intensity is[33]

$$I_{\mathrm{dir},l}(r_L)=\frac{W_l}{4\pi r_L^2}D. \tag{36}$$

The reverberant intensity is[43]

$$I_{\mathrm{rev},l}=\frac{4W_l}{S\bar{\alpha}}(1-\bar{\alpha})=\frac{4W_l}{R}, \tag{37}$$

where $R=S\bar{\alpha}/(1-\bar{\alpha})$ is the room constant, S is the room surface area and $\bar{\alpha}$ is the average sound absorption coefficient. Hence, the direct to reverberant sound intensity ratio is

$$\Delta = \frac{I_{\mathrm{dir},l}(r_L)}{I_{\mathrm{rev},l}} = \frac{DR}{16\pi r_L^2}. \tag{38}$$

This is equal to one at the critical distance $r_c = \sqrt{DR}/(4\sqrt{\pi})$.[33] Hence, to minimize reverberant effects in rooms, the loudspeaker should be positioned closer to the listener than the critical distance.

For an array that accurately reproduces the sound due to a point source at distance r_s, with power W_s, the direct intensity at the center of the array has the same form as Eq. (36) with $D=1$. The reverberant intensity produced by the array is $4W_{\mathrm{ext}}/R$ where W_{ext} is the total power radiated outward from the array into the room. Hence the general expression for the direct to reverberant ratio of a sound reproduction system is

$$\Delta = \frac{W_s}{W_{\mathrm{ext}}} \frac{R}{16\pi r_s^2}. \tag{39}$$

We now calculate the exterior power for the continuous and discrete array cases, and derive an approximate expression that applies at high frequencies which yields a simple interpretation in terms of the loudspeaker on-axis directivity D.

2. Exterior power for continuous and discrete array

At frequencies below the exterior Nyquist frequency, the sound radiated from a discrete implementation of the fixed-directivity array will be approximately equal to that of the continuous array. The acoustic power radiated can be computed by calculating the acoustic intensity from Eq. (26) and integrating over a sphere,[28] yielding

$$W_{\mathrm{ext}} = \frac{1}{2\rho c k^2} \sum_{n=0}^{\infty} \sum_{m=-n}^{n} \left| A_n^m \frac{a j_n(kr_L) - i(1-a) j_n'(kr_L)}{a h_n(kr_L) - i(1-a) h_n'(kr_L)} \right|^2. \tag{40}$$

Note that since the expansions in Eq. (5) and Eq. (10) apply for all angles, Eq. (40) includes the sound that propagates through the interior of the array to the exterior field. For the case of a point source with acoustic power W_s given in Eq. (6) the exterior power is (using the spherical harmonics addition theorem[30])

$$W_{\mathrm{ext}} = W_s \sum_{n=0}^{\infty} (2n+1) |h_n(kr_s)|^2 \times \left| \frac{\alpha j_n(kR) - i(1-\alpha) j_n'(kR)}{\alpha h_n(kR) - i(1-\alpha) h_n'(kR)} \right|^2. \tag{41}$$

At frequencies above the Nyquist frequency, the exterior power radiated from the discrete array must be calculated from the individual loudspeaker weights $\hat{w}_l$ or $\bar{w}_l$. Using the exterior field expansions in Eqs. (5) and (10), and Eq. (6), the radiated power for the weights $\hat{w}_l$ can be written

$$W_{\mathrm{ext}} = 4\pi W_s \sum_{n=0}^{\infty} |a j_n(kr_L) - i(1-a) j_n'(kr_L)|^2 \times \sum_{m=-n}^{n} \left| \sum_{l=1}^{L} \hat{w}_l Y_n^m(\theta_l, \phi_l)^* \right|^2. \tag{42}$$

3. High frequency approximation

Equation (42) can be approximated by noting that at high frequencies the power radiated from the array will tend to the sum of the powers radiated from each loudspeaker, although interference effects will still occur. Since each loudspeaker is assumed to have the same power as the source, with an amplitude weighting factor ($\hat{w}_l$ for example), the exterior power is approximated by

$$W_{\mathrm{ext}} \approx \frac{W_s}{D} \sum_{l=1}^{L} |\hat{w}_l|^2 = \frac{r_L^2}{r_s^2} \frac{W_s}{D} \sum_{l=1}^{L} |\tilde{w}_l|^2, \tag{43}$$

where the normalized weights

$$\tilde{w}_l = \frac{r_s}{r_L} \hat{w}_l \tag{44}$$

are defined by noting that the sound pressure produced by the array at the origin must satisfy

$$\sum_{l=1}^{L} \hat{w}_l(\theta_s, \phi_s) = \frac{r_L}{r_s} e^{ik(r_s - r_L)}. \tag{45}$$

Note that Eq. (43) also includes the sound that propagates through the interior of the array and to the exterior field. Substituting Eq. (43) into Eq. (39), the direct to reverberant ratio at high frequencies can be written

$$\Delta_{\mathrm{high}} \approx \frac{DR}{16\pi r_L^2} \frac{1}{\sum_{l=1}^{L} |\tilde{w}_l|^2}. \tag{46}$$

This has a similar form to Eq. (38) with an additional term due to the loudspeaker weights. The DRR is reduced if the sum of the squared normalized loudspeaker weights is greater than one. The term

$$\gamma = \sum_{l=1}^{L} |\tilde{w}_l|^2 \tag{47}$$

is thus a figure of merit for any sound reproduction design above the exterior Nyquist frequency of the array. Solutions for which γ is large have been shown to be non-robust solutions for which large errors in the reproduced field can occur for small perturbations in the loudspeaker positions and frequency responses.[40] For robust solutions, γ is ideally one or less in which case the direct to reverberant ratio is the same or better than that of a single directional loudspeaker at a distance r_L.

IV. SIMULATIONS

We now present simulations that allow the direct and mode-matched solutions to be assessed. We use a spherical array of 144 loudspeakers which are almost uniformly

arranged[31] at a radius of 1.5 m producing an exterior Nyquist frequency of 400 Hz. The loudspeaker array is assumed to be in a free field, so there are no room reflections.

The near-field of the loudspeaker dipole responses occur at a distance for which $k(r_L-r)=1$, which is a distance of 1.22 m at 200 Hz [Eq. (9)]. Due to the poor conditioning of the mode matching for the maximum possible mode order of 11 (see Fig. 4) and the need to maintain a high order for exterior control, we will use $N=10$ in the simulations. Both direct and mode matched solutions for $N=11$ produced higher weight energies, required larger regularization and produced higher errors than the tenth order solutions.

The desired field is that due to a point source positioned on the x-axis at $r_s=3$ m. In practice we found some variation in error performance versus source angle, but the relative performance of the two methods for $(\theta_s,\phi_s)=(\pi/2,0)$ is indicative of the behavior at other angles.

To quantify the performance of the fixed-directivity solutions we calculate the angle-averaged relative error between the desired field $p(r,\theta,\phi,k)$ and the reproduced field $\hat{p}(r,\theta,\phi,k)$ as follows:[10]

$$\bar{\varepsilon}(kr)=\frac{\int_{\Omega_r}|p(r,\theta,\phi,k)-\hat{p}(r,\theta,\phi,k)|^2d\Omega_r}{\int_{\Omega_r}|p(r,\theta,\phi,k)|^2d\Omega_r}. \tag{48}$$

This may be determined using the orthogonality properties of the spherical harmonic expansions in Eqs. (1), (5), and (10) as[12]

$$\bar{\varepsilon}(kr)=\frac{4\pi\sum_{n=0}^{\infty}j_n^2(kr)\sum_{m=-n}^{n}\left|\sum_{l=1}^{L}(iah_n(kr_L)+(1-a)h_n'(kr_L))\hat{w}_lY_n^m(\theta_l,\phi_l)^*-ih_n(kr_s)Y_n^m(\theta_s,\phi_s)^*\right|^2}{\sum_{n=0}^{\infty}(2n+1)j_n^2(kr)|h_n(kr_s)|^2}. \tag{49}$$

Figure 5 shows the exterior power relative to the source power as a function of frequency for $a=0.25$. At frequencies below the exterior Nyquist frequency (400 Hz), the radiated power equals the continuous array power. In the region of the Nyquist frequency the actual power deviates from the continuous result and at high frequencies, oscillates with frequency about the non-coherent power result.

Figure 6 shows the direct to reverberant ratios as a function of directivity parameter a for a room volume of 320 m^3 ($8\times8\times5$ m^3) with a mean room absorption of 0.2. At 200 Hz the exact (discrete array) DRR (solid line) equals the continuous array DRR (the two lines are identical) and the non-coherent result from Eq. (46) is incorrect. The non-coherent result is larger than the other two because at 200 Hz the sum of squared weights is approximately equal to one half, due to the increased near-field dipole response. At 400 Hz the discrete DRR and continuous DRR begin to diverge, and at 800 Hz the discrete DRR is approximately the same as the non-coherent DRR. The discrete DRR has a maximum of around 2.5 for a directivity parameter in the range of 0.25 to 0.3. This is consistent with the fact that the first-order loudspeaker directivity is maximum for $a=0.25$, and the variation from the 0.25 optimum is due to the coherent radiation from the array at low frequencies and the oscillatory variation of the actual exterior power at higher frequencies. For comparison, the DRR for a single loudspeaker in the same room at the loudspeaker radius has a maximum DRR of 2.55 for the hyper-cardioid response ($a=0.25$).

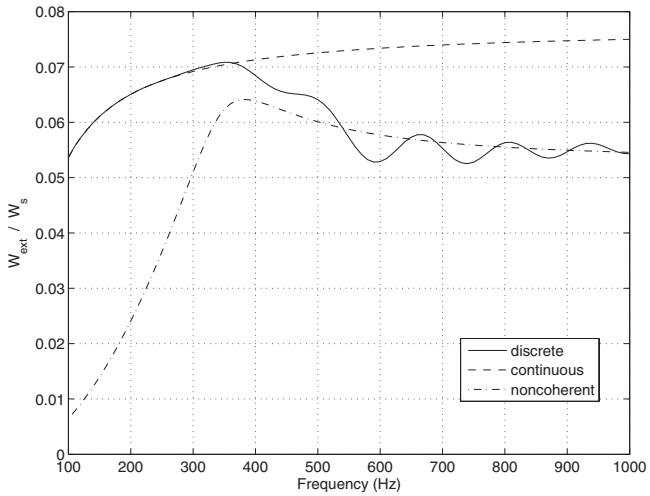

FIG. 5. Relative exterior power for a spherical array with $L=144$ loudspeakers, $r_L=1.5$ m, $a=0.25$, with the continuous array and high frequency approximation results shown for comparison.

Figures 7 and 8 show the real part of the sound field obtained from direct solution (25) at 200 Hz for $a=1$ (monopole loudspeakers) and $a=0.25$ (hyper-cardioid loudspeakers), respectively, assuming free-field conditions. (The corresponding mode-matched solution wave fields were similar in appearance, and their relative error performance is considered shortly.) The dashed circle indicates the loudspeaker radius and the dark circle is the maximum radius $r_N=(\sqrt{L}-1)/k$ where the mode-limited reproduction can maintain accuracy. The magnitude of the complex fields were limited to 1.5 times the expected magnitude at the origin, $1/(4\pi r_s)$, to make the images clearer. The monopole field produces sound radiation outwards from the array of the same amplitude as that radiating toward the center of array. This exterior radia-

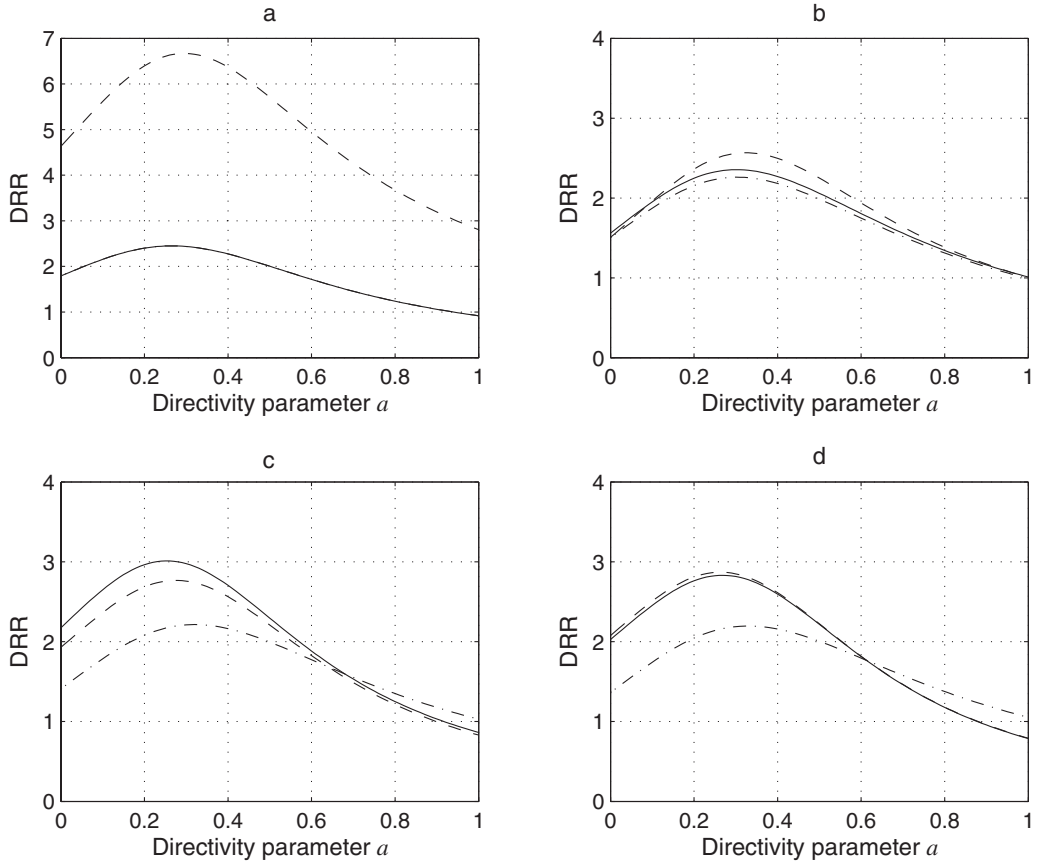

FIG. 6. Direct to reverberation ratio for a room volume of 320 m^3 and absorption coefficient 0.2. High frequency (non-coherent) DRR (dashed line), low-frequency continuous array DRR (dash-dotted line) and discrete array DRR (solid line), at frequencies 200 Hz (a), 400 Hz (b), 600 Hz (c) and 800 Hz (d).

tion would contribute high reverberant levels to the reproduced field when implemented in a room. The DRR for monopole sources with the same room conditions as Fig. 6 is 0.9. The hyper-cardioid field has a reduced exterior field compared to the monopole field, with a DRR for the same room conditions as Fig. 6 of 2.6, an improvement by a factor of 3.2 over the monopole source case. However, the accuracy of the reproduced field is reduced for radii near r_L. There is thus a slight trade-off between exterior radiation and interior

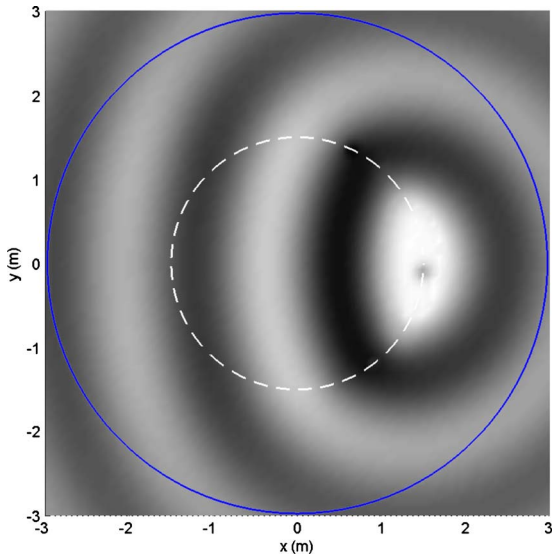

FIG. 7. (Color online) Reproduced sound field in free-field conditions, f =200 Hz, r_L=1.5 m, r_s=3 m, a=1.0 (monopole sources). The dark line denotes the maximum radius where accurate field reconstruction is possible, and the dashed white line is the loudspeaker radius.

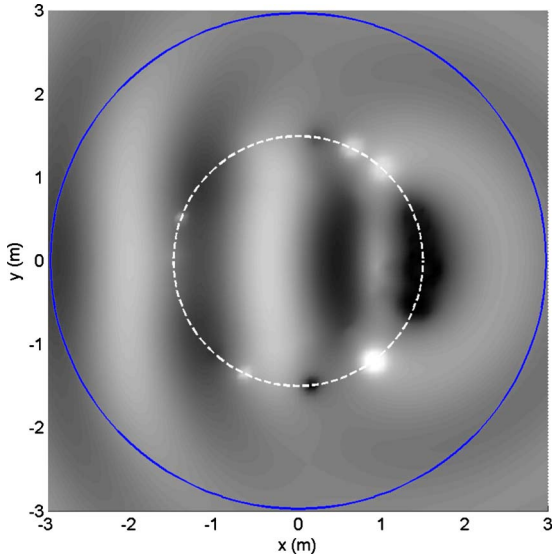

FIG. 8. (Color online) Reproduced sound field in free-field conditions, f =200 Hz, r_L=1.5 m, r_s=3 m, a=0.25 (hyper-cardioid sources). The dark line denotes the maximum radius where accurate field reconstruction is possible, and the dashed white line is the loudspeaker radius.

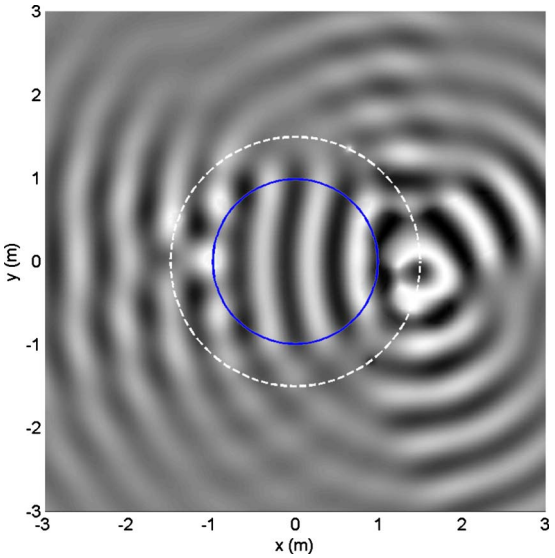

FIG. 9. (Color online) Reproduced sound field in free-field conditions, $f=600$ Hz, $r_L=1.5$ m, $r_s=3$ m, $a=1.0$ (monopole sources). The dark line denotes the maximum radius where accurate field reconstruction is possible, and the dashed white line is the loudspeaker radius.

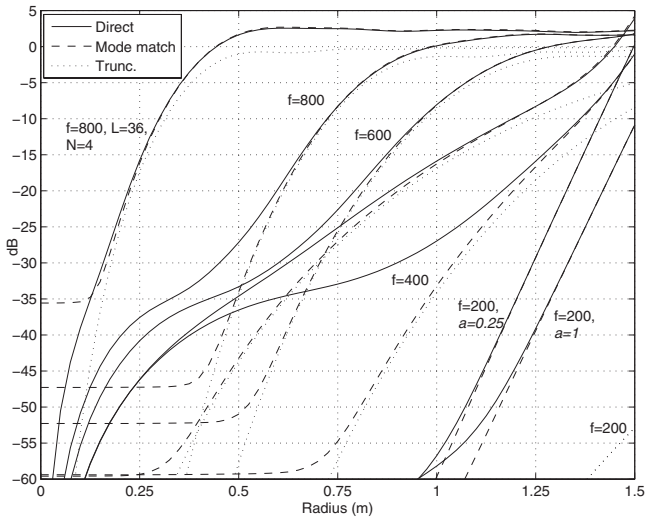

FIG. 11. Direct and mode-matched angle-averaged relative error in free field conditions from Eq. (49) at $f=200$, 400, 600 and 800 Hz, $a=0.25$, $r_L=1.5$ m, $r_s=3$ m, $N=10$. The error at $f=200$ Hz with $a=1$, and the error at $f=800$ Hz for $L=36$ loudspeakers and $N=4$, are also shown for comparison. The monopole source truncation error for $N=10$ is also shown.

accuracy at low frequencies when using directional loudspeakers.

Figures 9 and 10 shows the sound fields produced by monopole and hyper-cardioid loudspeakers, respectively, at a frequency of 600 Hz. In Figs. 7 and 8 the radius for accurate reproduction exceeds the loudspeaker radius and the sound field is accurate over the interior of the array, but the accuracy reduces near the loudspeakers, due to the modal truncation of the solutions. At 600 Hz the region of accuracy is about 1 m, and the field is inaccurate outside this radius for both monopole and hyper-cardioid cases. The fields within 1 m have similar accuracy, suggesting that there is little reduction in accuracy using the directional array above the Nyquist frequency.

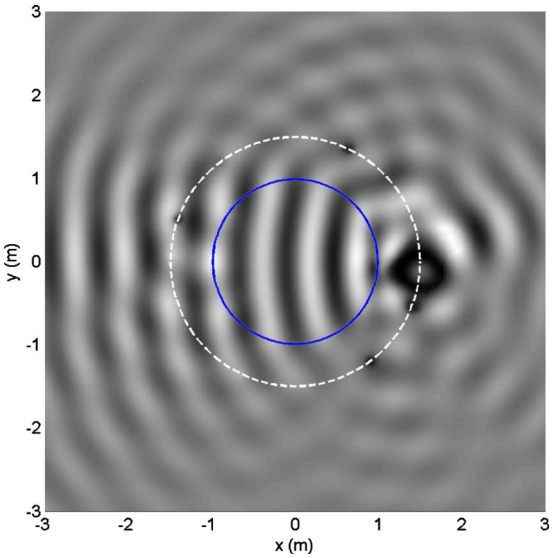

FIG. 10. (Color online) Reproduced sound field in free-field conditions, $f=600$ Hz, $r_L=1.5$ m, $r_s=3$ m, $a=0.25$ (hyper-cardioid sources). The dark line denotes the maximum radius where accurate field reconstruction is possible, and the dashed white line is the loudspeaker radius.

The monopole field displays greater beaming of exterior sound than the hyper-cardioid array, particularly at array positions nearest the source position. The DRR for the monopole array was 0.86, and for the hyper-cardioid array was 3.

With directional loudspeakers, the sound from the source angle propagates across the array and out the other side. If a listener walked around the outside of a directional loudspeaker array, he/she would tend to hear only those virtual sources originating from the far side of the array and would not tend to hear those originating from the near side.

Figure 11 shows the angle-averaged reproduction error calculated from Eq. (49) at frequencies 200, 400, 600 and 800 Hz, with $a=0.25$. Also shown for comparison is the radial error at 200 Hz for monopole sources, and the error for an array of $L=36$ hyper-cardioid loudspeakers.

At 200 Hz the error is below -30 dB for radii less than 1.25 and the accuracy is high over most of the array interior. The truncation error is significantly lower than the measured error, since at 200 Hz the error is increased by the near-field behavior of the loudspeaker dipole responses. The mode matched and direct solutions are essentially identical. The monopole array produces an error approximately 10 dB lower than the hyper-cardioid array which reduces the radius of accurate reproduction by around 7%, consistent with Fig. 7 and Fig. 8.

At 400 Hz the reproduction region is approximately equal to the loudspeaker radius. The mode matched solution remains close to the truncation error from 1.5 m down to 0.75 m, and for smaller radii, flattens out to a constant value of around -60 dB. The direct solution diverges more rapidly from the truncation error, but is below -30 dB for radii less than 0.85 m. Furthermore, the direct solution has no fixed error floor, and reduces to zero at the origin. The error curves at 600 and 800 Hz show similar behavior. It is clear that the mode-match solution is able to maintain accuracy out to a larger radius than the direct solution, and offers a more prac-

tical error performance, maintaining a fixed error floor from the center of the array out to the truncation error.

The angle-averaged error for 144 monopole sources at 600 Hz (not plotted in Fig. 11) is within 1 dB of the hypercardioid error at all radii. This is consistent with the similarity of the interior fields in Figs. 9 and 10. Hence, the directional array produces slightly lower accuracy near the loudspeaker radius at low frequencies, but has equivalent performance to the monopole array at higher frequencies.

The error at 800 Hz using $L=36$ hyper-cardioid loudspeakers shows that the region of accurate reproduction has reduced from $r=0.7$ to $r=0.3$ at an error of -10 dB. The maximum region for accurate reproduction is $r_N \approx (\sqrt{L}-1)/k$ [Eq. (15)], and so $L=36$ reduces the region of accurate reproduction to about 0.45 of the radius for $L=144$.

The figures of merit, Eq. (47), for both direct and mode-matched solutions with $L=144$ were $\gamma=2.57$ at 200 Hz (caused by the near-field behavior of the loudspeaker dipole responses), 0.98 at 400 Hz, 1.08 at 600 Hz and 0.98 at 800 Hz. Hence, above the near-field frequency f_d, the DRR is optimum.

V. CONCLUSIONS

This paper has investigated two methods for reproducing three-dimensional sound fields using loudspeakers with fixed, frequency-independent, first-order directivities, with the goal of reducing the reverberant field that occurs with sound reproduction in rooms. The reduction is quantified by the direct to reverberant sound ratio, which at low frequencies is governed by the coherent exterior field produced by the array, and at high frequencies is approximated by the individual behavior of each loudspeaker.

It has been shown that the reverberant field produced by a 3D spherical array can be reduced in a similar way to that due to a single loudspeaker and therefore directional loudspeakers are a useful approach to reducing room effects in sound field reproduction systems. The sound system does not need to be calibrated *in-situ* and is therefore simpler than adaptive systems. However, the reduction is likely to be less than that produced by an adaptive system. A further improvement in performance is possible at low frequencies by implementing a discrete approximation of the Kirchhoff-Helmholtz integral, which would eliminate the exterior field. This topic will be examined in a subsequent paper.

The large number of loudspeakers required for 3D sound field reproduction remains a challenge for any practical implementation. We have used 144 loudspeakers at a radius of 1.5 m in our simulations. The loudspeaker radius does not affect the region of accurate reproduction but practical systems would typically require a reduced number of loudspeakers, reducing the region of accurate reproduction, $r_N \approx (\sqrt{L}-1)/k$, at each frequency. Three-dimensional arrays are feasible in large specialized installations, such as public displays, but home use would typically require simpler 2D systems. The use of loudspeakers with directional characteristics also provides the prospect for higher quality 2D surround sound listening in the home. For example, vertical line sources with first-order directivity in azimuth would allow a significant reduction of the ceiling, floor and near-side wall reflections. Such loudspeakers can be built using a vertical line array with controlled radiation of the sound wave from the rear of each loudspeaker.[44] Higher-order 3D responses can be created using spherical arrays of transducers.[45]

We have assumed an ideal dipole response in this paper which has been equalized so that its response is flat beyond the near-field. The sound reproduction simulations assume these idealized dipoles in deriving the loudspeaker weights and in calculating the resulting sound field. In practice, dipole loudspeakers will not have a low frequency boost and therefore their near-field behavior will differ from the simulations. The simulations may be regarded as valid for all positions in the far-field of the loudspeakers, and the low-frequency performance of practical installations will differ from the results presented here.

ACKNOWLEDGMENT

M.P. would like to thank T. Betlehem for discussions during the course of this work.

[1] W. B. Snow, "Basic principles of stereophonic sound," J. SMPTE **61**, 567–589 (1953).
[2] H. Mertens, "Directional hearing in stereophony—Theory and experimental verification," E.B.U. Review – Part A **92**, 146–158 (1965).
[3] M. A. Gerzon, "Ambisonics in multichannel broadcasting and video," J. Audio Eng. Soc. **33**, 859–871 (1985).
[4] M. Gerzon, "Periphony: With-height sound reproduction," J. Audio Eng. Soc. **21**, 2–10 (1973).
[5] A. J. Berkhout, D. de Vries, and P. Vogel, "Acoustic control by wave field synthesis," J. Acoust. Soc. Am. **93**, 2764–2778 (1993).
[6] M. M. Boone, E. N. G. Verheijen, and P. F. Van Tol, "Spatial sound-field reproduction by wave-field synthesis," J. Audio Eng. Soc. **43**, 1003–1012 (1995).
[7] D. de Vries, "Sound reinforcement by wavefield synthesis: Adaptation of the synthesis operator to the loudspeaker directivity characteristics," J. Audio Eng. Soc. **44**, 1120–1131 (1996).
[8] M. A. Poletti, "A unified theory of horizontal holographic sound systems," J. Audio Eng. Soc. **48**, 1155–1182 (2000).
[9] O. Kirkeby and P. A. Nelson, "Reproduction of plane wave sound fields," J. Acoust. Soc. Am. **94**, 2992–3000 (1993).
[10] D. B. Ward and T. D. Abhayapala, "Reproduction of a plane-wave sound field using an array of loudspeakers," IEEE Trans. Speech Audio Process. **9**, 697–707 (2001).
[11] J. Daniel, "Spatial sound encoding including near field effect: Introducing distance coding filters and a viable new ambisonics format," AES 23rd International Conference, Copenhagen, Denmark (2003).
[12] M. A. Poletti, "Three dimensional surround sound systems based on spherical harmonics," J. Audio Eng. Soc. **53**, 1004–1025 (2005).
[13] S. Takane, Y. Suzuki, and T. Sone, "A new method for global sound field reproduction based on Kirchhoff's integral equation," Acta. Acust. Acust. **85**, 250–257 (1999).
[14] S. Ise, "A principle of sound field control based on the Kirchhoff-Helmholtz integral equation and the theory of inverse systems," Acta. Acust. Acust. **85**, 78–87 (1999).
[15] N. Epain and E. Friot, "Active control of sound inside a sphere via control of the acoustic pressure at the boundary surface," J. Sound Vib. **299**, 587–604 (2007).
[16] F. M. Fazi, P. A. Nelson, J. E. N. Christensen, and J. Seo, "Surround system based on three dimensional sound field reconstruction," AES 125th Convention, San Francisco, CA (2008), preprint 7555.
[17] F. M. Fazi and P. A. Nelson, "A theoretical study of sound field reconstruction techniques," Proceedings of the 19th International Congress on Acoustics, Madrid, Spain (2–7 September 2007).
[18] J. Ahrens and S. Spors, "An analytical approach to sound field reproduction using circular and spherical loudspeaker distributions," Acust. Acta Acust. **94**, 988–999 (2008).
[19] S. Spors, H. Buchner, R. Rabenstein, and W. Herbordt, "Active listening

room compensation for massive multichannel sound reproduction systems using wave-domain adaptive filtering," J. Acoust. Soc. Am. **122**, 354–369 (2007).
[20]P. A. Nelson, F. Orduna-Bustamante, and H. Hamada, "Multichannel signal processing techniques in the reproduction of sound," J. Audio Eng. Soc. **44**, 973–989 (1996).
[21]P. A. Nelson, H. Hamada, and S. J. Elliot, "Adaptive inverse filters for stereophonic sound reproduction," IEEE Trans. Signal Process. **40**, 1621–1632 (1992).
[22]T. Betlehem and T. Abhayapala, "Theory and design of sound field reproduction in reverberant rooms," J. Acoust. Soc. Am. **117**, 2100–2111 (2005).
[23]P.-A. Gauthier and A. Berry, "Adaptive wave field synthesis for sound field reproduction: Theory, experiments and future perspectives," J. Audio Eng. Soc. **55**, 1107–1124 (2007).
[24]P.-A. Gauthier, A. Berry, and W. Woszczyk, "Sound-field reproduction in-room using optimal control techniques: Simulations in the frequency domain," J. Acoust. Soc. Am. **117**, 662–678 (2005).
[25]S. Spors, M. Renk, and R. Rabenstein, "Limiting effects of active room compensation using wave field synthesis," AES 118th Convention, Barcelona, Spain, 28–31 May 2005, preprint 6400.
[26]L. Fuster, J. J. Lopez, A. Gonzalez, and P. D. Zuccarello, "Room compensation using multichannel inverse filters for wave field synthesis systems," AES 118th Convention, Barcelona, Spain, 28–31 May 2005, preprint 6401.
[27]M. Barron, *Auditorium Acoustics and Architectural Design* (E and F. N. Spon, London, 1993).
[28]E. G. Williams, *Fourier Acoustics* (Academic, San Diego, CA, 1999).
[29]E. Skudrzyk, *The Foundations of Acoustics* (Springer-Verlag, New York, 1971).
[30]D. Colton and R. Kress, *Inverse Acoustic and Electromagnetic Scattering Theory*, Applied Mathematical Sciences Vol. **93**, 2nd ed. (Springer, New York, 1998).
[31]http://www.personal.soton.ac.uk/jf1w07/nodes/nodes.html (Last viewed March 3, 2010).
[32]L. E. Kinsler, A. R. Frey, A. B. Coppens, and J. V. Sanders, *Fundamentals of Acoustics*, 4th ed. (Wiley, Hoboken, NJ, 1999).
[33]W. Anhert and F. Steffen, *Sound Reinforcement Engineering* (E and F.N. Spon, London, 1999).
[34]R. P. Glover, "A review of cardioid type unidirectional microphones," J. Acoust. Soc. Am. **11**, 296–302 (1940).
[35]F. M. Fazi, P. A. Nelson, and R. Potthast, "Analogies and differences between three methods for sound field reproduction," in Ambisonics Symposium 2009, Graz, Austria (2009).
[36]F. M. Fazi, P. A. Nelson, R. Potthast, and J. Seo, "An introduction to a generalised theory for sound field reproduction," *Proceedings of the 24th Conference of Reproduced Sound: Immersive Sound* (Institute of Acoustics, Brighton, UK, 20–21 November 2008), **30**(6), pp. 139–148.
[37]G. A. Daigle, M. R. Stinson, and J. G. Ryan, "Beamforming with air-coupled surface waves around a sphere and circular cylinder," J. Acoust. Soc. Am. **117**, 3373–3376 (2005).
[38]G. H. Golub and C. F. Van Loan, *Matrix Computations* (Johns Hopkins University Press, Baltimore, MD, 1983).
[39]L. L. Scharf, *Statistical Signal Processing: Detection, Estimation and Time Series Analysis* (Addison-Wesley, Reading, MA, 1991).
[40]M. A. Poletti, "Robust two-dimensional surround sound reproduction for nonuniform loudspeaker layouts," J. Audio Eng. Soc. **55**, 598–610 (2007).
[41]R. A. Horn and C. R. Johnson, *Matrix Analysis* (Cambridge University Press, Cambridge, 1985).
[42]A. Edelman, "Eigenvalues and condition numbers of random matrices," SIAM J. Matrix Anal. Appl. **9**, 543–560 (1988).
[43]L. L. Beranek, *Acoustics* (Acoustical Society of America, New York, 1993).
[44]M. M. Boone and O. J. Ouweltjes, "Design of a loudspeaker system with a low-frequency cardiodlike radiation pattern," J. Audio Eng. Soc. **45**, 702–707 (1997).
[45]B. Rafaely, "Spherical loudspeaker array for local active control of sound," J. Acoust. Soc. Am. **125**, 3006–3017 (2009).